



# Estimating time-dependent vegetation biases in the SMAP soil moisture product

Simon Zwieback<sup>1,2</sup>, Andreas Colliander<sup>3</sup>, Michael H. Cosh<sup>4</sup>, José Martínez-Fernández<sup>5</sup>, Heather McNairn<sup>6</sup>, Patrick J. Starks<sup>7</sup>, Marc Thibeault<sup>8</sup>, and Aaron Berg<sup>1</sup>

<sup>1</sup>Department of Geography, University of Guelph, Guelph, Ontario, Canada

<sup>2</sup>Department of Environmental Engineering, ETH Zurich, Zurich, Switzerland

<sup>3</sup>NASA Jet Propulsion Laboratory, California Institute of Technology, Pasadena, California, USA

<sup>4</sup>USDA-ARS Hydrology and Remote Sensing Laboratory, Beltsville, Maryland, USA

<sup>5</sup>Instituto Hispano Luso de Investigaciones Agrarias, Universidad de Salamanca, Salamanca, Spain

<sup>6</sup>Science and Technology Branch, Agriculture and Agri-Food Canada, Ottawa, Ontario, Canada

<sup>7</sup>USDA-ARS Grazinglands Research Laboratory, El Reno, Oklahoma, USA

<sup>8</sup>Comisión Nacional de Actividades Espaciales, Buenos Aires, Argentina

*Correspondence to:* Simon Zwieback ([zwieback@uoguelph.ca](mailto:zwieback@uoguelph.ca))

**Abstract.** Remotely sensed soil moisture products are influenced by vegetation and how it is accounted for in the retrieval, which is a potential source of time-variable biases. To estimate such complex, time-variable error structures from noisy data, we introduce a Bayesian extension to triple collocation in which the systematic errors and noise terms are not constant but vary with explanatory variables. We apply the technique to the SMAP soil moisture product over croplands, hypothesizing that errors in the vegetation correction during the retrieval leave a characteristic fingerprint in the soil moisture time series. We find that time-variable offsets and sensitivities are commonly associated with an imperfect vegetation correction. Especially the changes in sensitivity can be large, with seasonal variations of up to 40%. Variations of this size impede the seasonal comparison of soil moisture dynamics and the detection of extreme events. Also, estimates of vegetation-hydrology coupling can be distorted, as the SMAP soil moisture has larger  $R^2$  values with a biomass proxy than the in-situ data, whereas noise alone would induce the opposite effect. We conclude that complex biases can be present in soil moisture products and that they should be accounted for in observational and modelling studies.

## 1 Introduction

Soil moisture products derived from satellite measurements are subject to errors. These are not constant, but vary in space and time. For any given location, they may depend on variable factors such as vegetation phenology, atmospheric conditions or measurement characteristics like the incidence angle (Loew and Schlenz, 2011; Entekhabi et al., 2010; Su et al., 2016). Vegetation is commonly considered to be the most delicate factor to control when retrieving soil moisture from the raw satellite measurements (Dorigo et al., 2017; Chan et al., 2016). An imperfect vegetation correction during the retrieval will induce time-variable errors in the soil moisture product (Konings et al., 2017). As such structural errors potentially distort estimates



of vegetation-soil moisture coupling in unexpected ways (cf. Doherty and Welter, 2010), they are more pernicious than simple quasi-random noise or than time-constant biases.

However, the time-variable error properties of soil moisture products are poorly understood and rarely considered in practice (Loew and Schlenz, 2011). Arguably one reason for this is that there is currently no consistent way of estimating such rich error structures from data. If an exact reference soil moisture measurement were available, this would be an easy enterprise (Su and Ryu, 2015). Dense in-situ measurements are widely considered to be the closest one can get to perfect reference data, but they are rare, and non-negligible uncertainties remain (Colliander et al., 2017). In absence of perfect reference data, any useful error estimation procedure must cope with errors in all input data. Triple collocation and its various extensions can provide consistent error estimates in these circumstances (Gruber et al., 2016; Zwieback et al., 2016). However, similar to the standard RMSE metric they cannot directly separate non-constant systematic errors from quasi-random measurement noise. Conversely, common pre-processing steps (forming anomalies, analysis of short time periods) provide a simple means to deal with certain non-constant errors but lack generality (Loew and Schlenz, 2011; Gruber et al., 2016).

Here, we extend triple collocation to estimate non-constant error structures (Sec. 2). The central idea is to express systematic errors such as an offset and random errors in terms of explanatory variables like a vegetation index (cf. Xu et al., 2017; Doherty and Welter, 2010). The choice of explanatory variables should be informed by the measurement principle and the retrieval algorithm. In our case study of the SMAP product, we will specify it in terms of a misspecification of the vegetation input during the retrieval process. We generally assume that three independent and noisy products are available. Once their hypothesized error structure has been specified, our Bayesian Triple Collocation approach proceeds in two steps. First, the specified error structure is embedded in a probabilistic model that links the unknown soil moisture  $\theta$  with observed soil moisture products  $y_n$ . Second, Bayesian inference is applied, and one thus obtains estimates and uncertainties of the error parameters of interest. A simulation study indicates that time-variable systematic errors can be estimated reliably for as few as 250 samples (Sec. 3).

We apply this procedure to estimate time-variable biases in the SMAP soil moisture product that are associated with an imperfect vegetation correction (Sec. 4). This is not to say that other soil moisture products are not subject to similar biases; on the contrary, the SMAP baseline product is widely considered to provide the most reliable global soil moisture data record available (Chan et al., 2017; Colliander et al., 2017). To estimate soil moisture from the passive microwave measurements, the retrieval algorithm has to correct for the vegetation influence (Kurum et al., 2011; Chan et al., 2017). Specifically, the SMAP algorithm assumes that the vegetation optical depth  $\tau$ , a dimensionless measure of how much the microwaves interact with the vegetation, is known a priori.

We focus on croplands, as they present a particular challenge to the vegetation correction approach using an a priori  $\tau$ . Over crops, the input  $\tau$ , which is derived from the Normalized Difference Vegetation Index (NDVI), only provides an incomplete picture of the vegetation influence at microwave frequencies. The NDVI, being strongly influenced by leaf chemistry, can only indirectly account for the dominant controls on  $\tau$ , namely the vegetation water content and the canopy structure, both of which are particularly diverse and dynamic in crops (Lawrence et al., 2014; Konings et al., 2017). The NDVI-based input  $\tau$  also does not account for inter-annual variability in vegetation conditions, which cannot be neglected over croplands (Patton and Hornbuckle, 2013). Consequently, agricultural regions have been identified as a weak spot for the SMAP product (Colliander



et al., 2017). However, the time-average metrics analysed so far cannot distinguish seasonal biases from quasi-random noise, and the magnitude of vegetation-induced systematic errors thus remains unknown.

We hypothesize that seasonal changes in the error structure arise due to an inaccurate vegetation correction in the retrieval, so that the biases relative to the in-situ data track the misspecification in the vegetation optical depth  $\Delta\tau$ . We specify the SMAP offset and sensitivity as a function of  $\Delta\tau$ , based on predictions by the  $\tau$ - $\omega$  radiative transfer model (Kurum et al., 2011). We estimate the associated error parameters with the Bayesian triple collocation approach, using in-situ and re-analysis data as additional soil moisture products. We find that SMAP soil moisture biases that track  $\Delta\tau$  are widespread and large over croplands. This is especially so for the sensitivity, resulting in a time-dependent dynamic range of the SMAP soil moisture product that impedes seasonal comparisons of soil moisture dynamics. We attribute the time-variable biases to the imperfect vegetation correction, as the inferred bias characteristics largely match those predicted by the  $\tau$ - $\omega$  model. To illustrate the potential influence of these biases on estimates of vegetation-hydrology coupling (Adegoke and Carleton, 2002), we show that the coefficient of determination between SMOS  $\tau$  anomalies and SMAP soil moisture anomalies is inflated compared to in-situ soil moisture measurements. In summary, our analyses suggest that soil moisture products can be subject to previously neglected time-variable biases that should be accounted for in observational and modelling studies.

## 2 Bayesian triple collocation

We now present a general overview of the approach (Fig. 1), which consists of two components. First, a probabilistic model that links the unknown soil moisture  $\theta$  with the observed soil moisture products  $y_n$ . The link itself characterizes the error structure: it depends on error parameters  $\gamma_{y_n}$  and explanatory variables  $w$ . Second, a Bayesian inference approach that provides estimates of all the unknown quantities, in particular the error parameters. By conditioning on the observed soil moisture data (input), we get a posterior distribution over the unobservable quantities (output). We focus on a setting inspired by triple collocation studies, i.e. we for the most part assume that  $N = 3$  independent and noisy products are available (Gruber et al., 2016).

Our approach has several characteristics that make it useful in a wide range of applications. It is widely applicable, as no soil moisture product is assumed to be free of errors. This is particularly critical for estimating the noise magnitude and the sensitivity, which cannot be estimated consistently by standard regression approaches when the reference product is subject to errors (Yilmaz and Crow, 2013). Also, it provides principled uncertainty estimates through the posterior distribution. It is flexible, as it can be adapted to many functional relations and error structures. Finally, it is transparent because all modelling assumptions are explicit. Owing to its flexibility, the model can be modified to test the sensitivity of the results to certain assumptions. We will exploit these advantages by modifying the prior distribution and the likelihood; for instance, we will test several models for the unknown soil moisture  $\theta$ .

### 2.1 Probabilistic model

The probability distribution comprises the observable products  $y_0$  to  $y_{N-1}$ , the unknown soil moisture  $\theta$  and numerous parameters: the set of parameters  $\gamma_{y_n}$  characterizes product  $n$ , and  $\gamma_\theta$  does the same for the soil moisture. The structure of the model

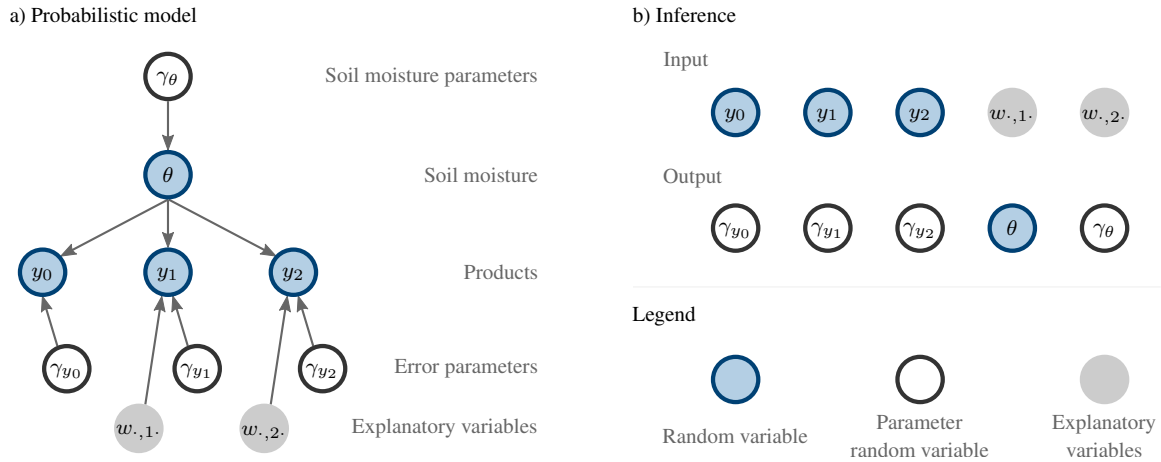


**Figure 1.** The two components of Bayesian triple collocation. a) The probabilistic model expresses the observable products in terms of the unknown soil moisture, error parameters and explanatory variables. The set of error parameters of the reference product,  $\gamma_{y_0}$ , does not contain variable bias terms. b) The soil moisture products and explanatory variables serve as input to the inference, which produces estimates (posterior probability distributions) of, amongst other things, the error parameters.

is summarized in Fig. 1a, which depicts the corresponding directed acyclic graph (MacKay, 2003). This graph expresses how the distribution over all the random variables is factorized into smaller components. Starting with an observable product  $y_n$ , its distribution is modelled conditional on the unknown  $\theta$ , the associated parameters  $\gamma_{y_n}$  (including the time-independent and time-dependent bias parameters) and the explanatory variables  $w_{.,n}$ . We refer to this conditional distribution as the error model.

5 It is conditional on the soil moisture  $\theta$ , whose distribution (conditional on parameters  $\gamma_\theta$ ) is referred to as the soil moisture model. The final component are the parameters  $\gamma_{y_n}$  and  $\gamma_\theta$ , which are assigned prior distributions. These prior distributions are integral to the Bayesian approach, and they express the initial belief about the parameters' likely values. We now describe each of these components in turn. To facilitate future applications of the approach, we do this using very general notation, which we will later in the SMAP case study simplify by dropping subscripts.

### 10 2.1.1 Error model

Each product's error model is governed by a set of parameters  $\gamma_{y_n}$  which quantify the error component such as the biases (systematic errors). We consider an affine error model according to which the dynamic range or sensitivity of the product can differ from that of the true soil moisture, governed by the scaling parameter  $L_n(t)$ . We also include an additive offset or bias  $M_n(t)$  (Zwieback et al., 2012; Yilmaz and Crow, 2013), yielding

$$15 \quad y_n(t) = L_n(t) (\theta(t) - \theta_0) + (\theta_0 + M_n(t)) + \epsilon_n(t), \quad (1)$$

where we essentially relate the deviation of soil moisture from a typical, prescribed soil moisture  $\theta_0$  to the observed product.



Our key extension compared to previous triple collocation studies is to make the bias terms and the noise magnitude vary with time-dependent explanatory variables,  $w_{\cdot,np}(t)$ :

$$L_n(t) = l_n + \sum_{p=1}^{P_{\lambda,n}} \lambda_{np} w_{\lambda,np}(t) \quad (2)$$

$$M_n(t) = m_n + \sum_{p=1}^{P_{\mu,n}} \mu_{np} w_{\mu,np}(t) \quad (3)$$

- 5 where  $l_n$  and  $m_n$  are time-invariant values specific to product  $n$ , and the parameters  $\lambda_{np}$  and  $\mu_{np}$  are coefficients that quantify the sensitivity to the explanatory variable  $w_{\lambda,np}$  and  $w_{\mu,np}$ , respectively. These variables are external quantities that are part of the model input. To facilitate the interpretation of the parameters, we always assume the explanatory variables to have zero mean and unit standard deviation (Gelman et al., 2008).  $l_n$  and  $m_n$  thus represent the time-average biases. The magnitude of  $\lambda_n$  and  $\mu_n$  represents the magnitude of the associated temporal changes in  $L_n$  and  $M_n$ , respectively.
- 10 The quasi-random errors are characterized by their variance and further distributional assumptions. For the variance  $S_n^2(t) = E(\epsilon_n(t)^2)$  we suggest a multiplicative model that is commonly employed in regression studies (Harvey, 1976)

$$S_n^2(t) = \sigma_n^2(t) \prod_{p=1}^{P_{\sigma,n}} w_{\sigma,np}(t)^{\kappa_{np}} \quad (4)$$

- where  $\kappa$  governs the sensitivity of the error variance to the explanatory variable, which has to be positive. We always assume it to be normalized so its geometric mean is one, as this simplifies the interpretation of the typical variance  $\sigma_n^2(t)$ . A positive value  $\kappa > 0$  indicates a larger variance as the explanatory variable increases, and a negative value corresponds to a smaller variance.
- 15 To complete the specification of the errors, a probability distribution has to be assumed. We focus on a normal distribution with zero mean and variance given by  $S_n^2$ , as our robustness checks indicated that the results were not very sensitive to this assumption (cf. Sec. 3). Finally, two further properties have to be specified. First, we assume that the errors at different times are independent. We will later show that violations of this assumption commonly have negligible impact on the estimated parameter values. Second, we postulate that the errors of the various products are independent. This is generally a key assumption in triple collocation-type studies (Gruber et al., 2016).

- We generally specify  $y_0$  to be the reference product (Yilmaz and Crow, 2013; Gruber et al., 2016). Its error magnitude is assumed to be constant over time, and so are its additive bias ( $M = 0 \text{ m}^3 \text{ m}^{-3}$ ) and its sensitivity  $L = 1$ . This constraint ensures that the unknown soil moisture distribution (its mean and scale) can be inferred from data, as it essentially specified what the reference product was a noisy estimate of (Zwieback et al., 2016). The bias terms are thus always relative to this reference product.

### 2.1.2 Soil moisture model

The second piece of the probabilistic model concerns the soil moisture  $\theta$ , the distribution of which also has to be specified. Our default representation is a simple logistic model. The physical quantity  $\theta$ , which is constrained to between 0 and the porosity



**Table 1.** The default model specification used in both the simulation study and the SMAP case study, and the baseline configuration for the simulation runs. The bias terms for the reference product  $y_0$  were assumed known.

	Model specification	Simulation parameters
Errors		
$\sigma$ [ $\text{m}^3 \text{m}^{-3}$ ]	exponential prior	[0.02, 0.04, 0.05]
$m$ [ $\text{m}^3 \text{m}^{-3}$ ]	Student prior	$m_0 = 0$ [0.00, 0.03, -0.05]
$l$ [-]	Student prior	$l_0 = 1$ [1.0, 1.1, 0.9]
$\mu$ [ $\text{m}^3 \text{m}^{-3}$ ]	Student prior	$\mu_0 = 0$ [0.0, 0.02, -0.02]
$\lambda$ [-]	Student prior	$\lambda_0 = 0$ [0.0, 0.06, 0.0]
$\kappa$ [-]	Student prior	$\kappa_0 = 0$ [0.0, 0.2, -0.2]
Ancillary components		
$\epsilon$ distribution	Normal	Normal
$\theta$ distribution	logistic ( $A, B, \phi$ )	logistic

$\phi$ , is expressed as a function of the non-dimensional unbounded soil moisture  $\Theta$

$$\theta(t) = \phi \frac{1}{1 + \exp(-A - B\Theta(t))} \text{ with } \Theta \sim \mathcal{N}(0, 1). \quad (5)$$

$\Theta$  is modelled as a standard normal random variable. The site-specific parameters  $A$ ,  $B$  and  $\phi$  are inferred in the Bayesian inference. We summarized the parameters of the soil moisture model under  $\gamma_\theta$ .

- 5 One drawback of this model is that it cannot account for the autocorrelation and seasonality of soil moisture. To test for the importance of temporal characteristics, we also generalize the model by making  $A$  and  $B$  time dependent. We do this by expanding  $A$  and  $B$  in a spline basis with 12 monthly basis functions. While this model cannot completely account for the complex temporal characteristics of soil moisture, it captures the seasonal trends.

### 2.1.3 Prior distributions

- 10 To complete the full probability distribution, one has to specify the prior distributions of the parameters  $\gamma_\theta$  and  $\gamma_{y_n}$ . As we work with normalized explanatory variables, we can use a problem-independent prior distribution (Gelman et al., 2008). We choose the priors to be weakly informative, thus partially ruling out unreasonable values but still letting the data speak for themselves (Gelman et al., 2008). Our default choices are summarized in Tab. 1.

- 15 For all products  $y_n$ , we put a very weak prior on the error magnitude variance  $\sigma^2$ . It is given by an exponential distribution with mean  $0.1 (\text{m}^3 \text{m}^{-3})^2$ . In other words, we barely constrain this quantity. For the product error parameters,  $m$  and  $\mu$  [ $\text{m}^3 \text{m}^{-3}$ ] are assumed distributed according to a t distribution  $T(0, 0.3^2; 4)$ . It is centred at 0 with a standard deviation of 0.3 and very heavy tails due to its four degrees of freedom. These values barely constrain the estimation of the additive bias  $m$ , as they do not rule out biases as large as  $0.5 \text{m}^3 \text{m}^{-3}$ . Similarly for  $l$  and  $\lambda$  [-], whose prior is  $T(1, 0.3^2; 4)$ .



The standard prior distribution for the soil moisture parameters  $\gamma_\theta$  follows a similar logic. The porosity [ $\text{m}^3 \text{m}^{-3}$ ] is given by  $T(0.4, 0.1^2; 4)$ . The parameters  $A$  and  $B$  in the standard logistic model are assigned  $T(0, 3.0^2; 4)$  and an exponential distribution with mean 3.0, respectively.

## 2.2 Bayesian inference

5 The Bayesian inference takes the observed products and explanatory variables as input and outputs posterior probability distributions over the unknown quantities (Fig. 1). The posterior distributions are obtained from the probabilistic model by conditioning on the input data. Conditioning is a well-defined mathematical operation, but analytical solutions are infeasible for complicated models like ours (MacKay, 2003). Instead, one has to resort to approximations. Monte Carlo methods are arguably the most popular. Their output is an approximation to the posterior distribution that consists of samples drawn from this distribution. Here, we rely on Hamiltonian Monte Carlo as implemented using the adaptive No-U-Turn Sampler in pymc3 (Hoffman and Gelman, 2014; Salvatier et al., 2016). We sample two independent chains with 2000 samples each, which standard quality controls (divergences, chain mixing) indicate is sufficient. Following common practice, the first 1000 samples are discarded (Brooks and Gelman, 1998)

## 3 Simulation study

15 We now study the applicability of Bayesian triple collocation using a simulation study. We used three simulated products with realistic error properties (Tab. 1).  $y_0$  was taken to be the reference product in both the simulation and in the probabilistic models. For the other two products the biases and error magnitudes were assumed dependent on a normalized explanatory variable that varied seasonally (Tab. 1). The soil moisture was prescribed using a simple antecedent precipitation model driven by a seasonally-dependent Hidden Markov Model rainfall generator, which gave rise to autocorrelated soil moisture. Mimicking the SMAP sensor, an observation was made every 2-4 days.

We first analysed the fidelity with which the error parameters could be estimated. To this end, we simulated 25 time series and computed the posterior distribution using the default probability model of the previous section, summarized in Tab. 1. We computed an RMSE error by comparing the prescribed parameters with the posterior mean inferred from each simulation run. To explore the impact of the number of observations on the accuracy, we did this for 100, 250 and 500 observations, which bound the number of observations that were available in the SMAP study.

The error parameters could be estimated with sufficient fidelity in the simulation study (Fig. 2; full model). The accuracy of the estimated time-variable additive bias parameter  $\mu$  was found better than  $0.01 \text{ m}^3 \text{ m}^{-3}$ , and thus likely sufficient to detect relevant non-constant biases. The sensitivity coefficients  $\lambda$  are retrieved with comparable precision: the RMSE of 0.05 corresponds to a differential bias between dry and wet conditions of around  $0.01 \text{ m}^3 \text{ m}^{-3}$ . Again, this should be sufficient for many applications. Finally, the time-constant noise magnitude  $\sigma$  could be estimated accurately ( $\ll 0.005 \text{ m}^3 \text{ m}^{-3}$ ).

Bayesian triple collocation yields a distribution of the parameters and thus naturally provides uncertainty estimates. These compare favourably to the RMSE errors: Fig. 2b shows that the posterior standard deviations are within 10 to 20 % of the



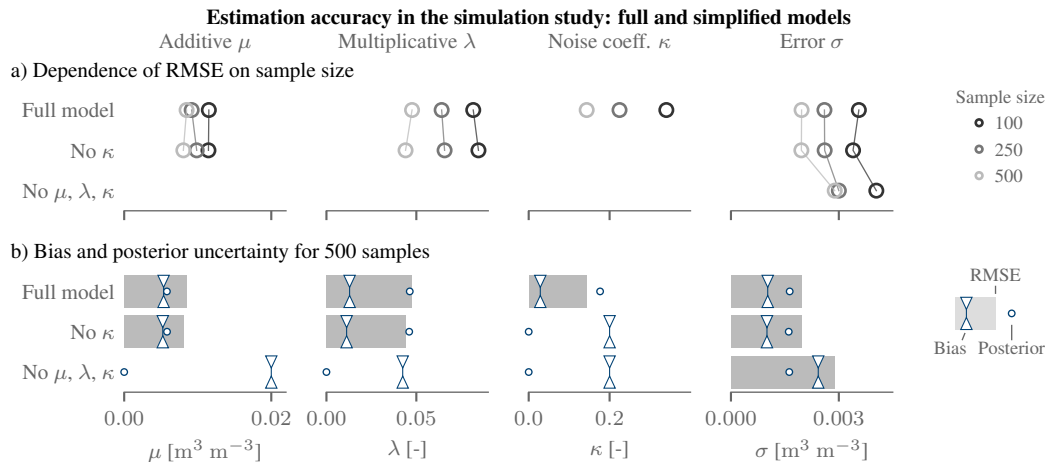


**Figure 2.** Simulation results illustrating the estimation fidelity. a) Dependence on sample size. b) Comparison of RMSE and bias to the posterior standard deviation. In a) and b) the first line shows the full model, whereas  $\kappa$  is set to zero in the inference in the second, and  $\lambda$ ,  $\mu$  and  $\kappa$  were set to zero in the third.

RMSE errors. Even though these two quantities represent different kinds of uncertainty, they are expected to be comparable for large samples (MacKay, 2003). The posterior distribution hence provides a useful summary of the estimation uncertainty.

To test the sensitivity of the estimates to model assumptions, we extended the simulation study. The most critical aspect turned out to be the specification of the bias terms: neglecting variable bias terms can impair the overall estimation quality.

5 Neglecting the complex error structure leads to an overestimation of the error magnitude (Fig. 2). In our case, setting  $\mu$ ,  $\lambda$  and  $\kappa$  to 0 induced an increase in the RMSE of  $\sigma$  by a factor of two. This increase was mainly due to a large bias, as the varying offsets were wrongly attributed to quasi-random noise. The posterior uncertainty estimates also became inaccurate. Conversely, neglecting only the variability of the error magnitude (i.e. setting  $\kappa = 0$ ) had limited impact on the retrieval of the other parameters.

10 To test for additional model assumptions, we modified the model and the forward simulations. The impact on the estimation accuracy was typically limited (see the supplement), so we only provide a short summary. First, the model for the noise term  $\epsilon$  had a moderate influence on the estimation quality. A mismatch between assumed and simulated  $\epsilon$  distributions increased the RMSE of the error variance by a small amount ( $<0.001 \text{ m}^3 \text{m}^{-3}$  for  $\sigma$ ) for a range of error distributions and strongly autocorrelated errors. The other crucial assumption in the model is the probability distribution for the soil moisture. Also here,

15 the changes are typically small (up to 10% improvement in the RMSE) when replacing the standard time-invariant model by a seasonally variable model or by a different time-invariant model. The prior distributions had an even smaller impact. Making the prior distributions twice as wide or the tails less heavy changed the estimates by only a few percent.





**Table 2.** Network sites from north to south, including their Koeppen-Geiger climate regime.

Site	Location	Climate	Crop cover [%]	Samples
Kenaston	Canada (Saskatchewan)	Cold	90	351
Carman	Canada (Manitoba)	Cold	80	352
South Fork	USA (Iowa)	Cold	90	323
REMEDHUS	Spain	Temperate	80	475
Fort Cobb	USA (Oklahoma)	Temperate	60	413
Bell Ville	Argentina	Arid	90	399
Monte Buey	Argentina	Arid	90	400

## 4 SMAP case study

### 4.1 Materials and methods

#### 4.1.1 Data

We analysed the SMAP enhanced Level-2 soil moisture product, which is disseminated on the 9 km EASE-Grid 2.0 at a resolution of 33 km (Chan et al., 2017; O' Neill et al.). It contains a variety of estimates of the top (5 cm) soil moisture, of which we chose the standard product (baseline V single channel algorithm, 9 am morning passes). The single channel retrievals rely on an a priori  $\tau$  derived from a MODIS climatology; these  $\tau$  values are included in the disseminated product. We studied all available data since the beginning of the record in April 2015 until August 2017, i.e. up to three annual growing seasons. After removing flagged retrievals (Colliander et al., 2017), the number of available measurements is on the order of 300-500, which is not ideal but should be sufficient according to Fig. 2a.

The analyses focus on seven locations in North America, South America and Europe with significant crop cover, due to the availability of high-quality dense in-situ networks (Tab. 2). At these SMAP core or candidate sites, continuous calibrated in-situ measurements at 5 cm depth are collected at multiple locations within a SMAP grid cell (Colliander, 2017; Colliander et al., 2017).

To provide a better overview of the spatial patterns, we also used data from > 200 in-situ sites in the contiguous United States (SCAN and USCRN networks). These sparse sites consist of a single station per satellite pixel, and their representativeness is hence not comparable to that of the network sites. The USDA's SCAN network has been in continuous operation since 1999 and provides soil moisture data at 2 in (5 cm) depth (Schaefer et al., 2007). The USCRN network consists of 114 sites whose location was chosen to be maximally representative of its surroundings; we used the 5 cm soil moisture observations (Bell et al., 2013; Diamond et al., 2013; Palecki et al., 2017). We assigned these sites a dominant land cover based on the MODIS MCD12C1 land cover product (Friedl et al., 2017).

For the third soil moisture product we used the MERRA2 reanalysis (M2T1NXLND.5.12.4) (Gelaro et al., 2017; Global Modeling and Assimilation Office, 2017). It is the most recent reanalysis product of NASA's Global Modeling Office, available



at a resolution of 55 km. For sensitivity analyses, we also used GLDAS-2 (Noah model, GLDAS\_NOAH025\_3H.2.1), a popular land assimilation data set (Roddell and Beaudoin, 2017).

To quantify the error structure as a function of  $\Delta\tau$ , we estimated  $\Delta\tau$  as the difference between an external estimate of  $\tau$  and the SMAP input  $\tau$ . The external estimate was based on independent L-band microwave observations by the SMOS satellite (Level 3 operational algorithm). The multi-angular observations and the temporal aggregation of multiple overpasses are conducive to providing robust, if noisy, measurements of the vegetation optical depth relevant to SMAP (Al Bitar et al., 2017). To reduce the impact of high-frequency noise, the  $\Delta\tau$  data were smoothed to a temporal resolution of 16 days (LOWESS filter). The explanatory variable used in the Bayesian inference is the normalized version

$$w_{\Delta\tau}(t) = \frac{1}{\text{std}(\Delta\tau)} (\Delta\tau(t) - \text{mean}(\Delta\tau)). \quad (6)$$

#### 10 4.1.2 Error estimation

In our estimation we specified the error structure based on our hypothesized impact of a vegetation misspecification. The  $\tau$ - $\omega$  model (Kurum et al., 2011) predicts that a vegetation misspecification  $\Delta\tau = \tau_{\text{inv}} - \tau_{\text{true}}$  will induce both a sensitivity  $L$  and an offset  $M$  which scale approximately linearly with  $\Delta\tau$  (Fig. 3a). There is thus only one explanatory variable ( $P_{\lambda,n} = P_{\mu,n} = 1$ ), namely the normalized  $w_{\Delta\tau}$  of Eq. 6. By slightly simplifying the notation, the error model reads

$$15 \quad y_{\text{SMAP}}(t) = \underbrace{(l + \lambda w_{\Delta\tau}(t))}_{L(t)} (\theta(t) - \theta_0) + \underbrace{(m + \mu w_{\Delta\tau}(t))}_{M(t)} + \theta_0 + \epsilon(t). \quad (7)$$

Here  $\theta_0$  was taken to be the mean value of the in-situ product. We quickly recall the interpretation of the error parameters.  $\lambda$  and  $\mu$  quantify the temporal changes in the sensitivity and offset, respectively, that are associated with changes in  $\Delta\tau$ . Their magnitudes correspond to the temporal standard deviation of the sensitivity and offset, respectively (Fig. 3b). Their sign expresses the direction of the dependence on  $\Delta\tau$ . It is predicted to be positive: as  $\Delta\tau$  grows, the inversion increasingly overcompensates the vegetation-induced loss of sensitivity to soil moisture and increase in brightness temperature, which in turn inflates both  $L$  and  $M$ , respectively.

The same overcompensation also increases the noise level, so that we also made the variance of  $\epsilon(t)$ ,  $S^2(t)$ , time dependent. We used two explanatory variables,  $\exp \Delta\tau$  and the external  $\tau$  (both normalized,  $P_{\kappa,n} = 2$ ). The reason for also including  $\tau$  was that the noise level  $S^2$  is predicted to depend on  $\tau$  even if  $\Delta\tau$  is constant, in contrast to the bias terms. By transforming  $\Delta\tau$  to  $\exp \Delta\tau$ , the predicted dependence of  $S^2$  shown in Fig. 3 could be reproduced accurately. The same error structure was assumed for the re-analysis data, whereas the in-situ observations were taken as reference product  $n = 0$ :  $L = 1$ ,  $M = 0$ ,  $\kappa = 0$ ). All other model components – the soil moisture and error distributions, the priors – are identical to the simulation study (Tab. 1).

30 To compare the estimated biases with the model predictions, we re-expressed  $\lambda$  and  $\mu$  in absolute terms by reversing the rescaling from  $\Delta\tau$  to  $w_{\Delta\tau}$ . Thus,  $\lambda^* = \lambda/\text{std}(\Delta\tau)$  is the slope of  $L$  vs  $\Delta\tau$ . In other words, it describes the change in  $L$  for

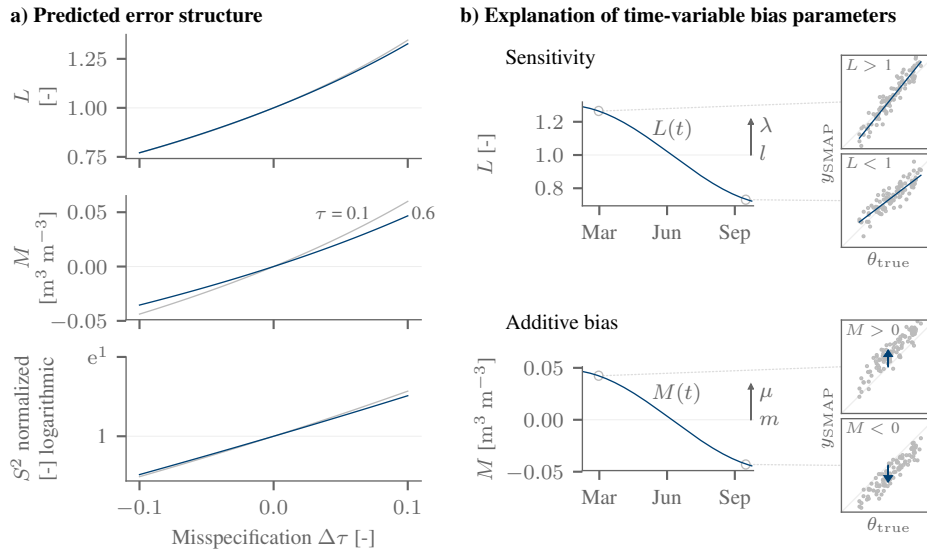


**Figure 3.** The expected error structure due to a misspecified vegetation in the SMAP retrieval. a) Additive bias  $M$ , sensitivity  $L$  and variable noise level  $S^2$  induced by a misspecified vegetation optical depth  $\tau$ , as predicted by the  $\tau$ - $\omega$  model for the SMAP satellite and single-scattering albedo  $\omega = 0.05$ . b) Explanation of the bias terms: a varying sensitivity  $L(t)$  changes the response of the SMAP retrieval to a unit change in the true soil moisture. The time-average value of  $L$  is  $l$ , and the temporal standard deviation of  $L$  is given by  $|\lambda|$  (length of arrow). A variable  $M$  induces non-constant offsets, and the magnitude of its temporal variability is given by  $|\mu|$ .

a unit change in  $\Delta\tau$ , and similarly for  $\mu^*$ . They can be directly compared to the model predictions in Fig. 3a. Note that the division only reverses the scaling but not the offset inherent in the normalization from  $\Delta\tau$  to  $w_{\Delta\tau}$ . Estimating the derivative at the mean value of  $\Delta\tau$  (due to the offset) rather than at  $\Delta\tau = 0$  has, however, no impact for a purely linear relation.

To test the robustness of the estimates, we varied the input data and the model configuration. Instead of using the SMOS  $\tau$  as reference, we also derived  $\Delta\tau$  from the SMAP dual channel (LOWESS smoothed) retrievals (O' Neill et al.) and from contemporaneous MODIS NDVI data (Didan, 2017). We converted the MODIS NDVI to  $\tau$  using the same equations as in the generation of the SMAP input climatology. We refer to these model runs as SMAP DC  $\tau$  and MODIS  $\tau$ , respectively. We also modified the external soil moisture products: instead of MERRA-2 we used GLDAS-2 (GLDAS  $\theta$ ), and we also dropped the reanalysis data set altogether (no reanalysis). This is possible in a Bayesian setting; to improve the identification of the errors, we assigned a narrower prior distribution to the in-situ noise magnitude ( $0.02 \text{ m}^3 \text{m}^{-3}$ ). Finally, we also modified the model configuration in two ways. First, we used a homoscedastic error model, i.e. we set all  $\kappa = 0$ . Second, we made the probability model for  $\theta$  vary seasonally as described in Sec. 2.1.2, referred to as  $\theta$  spline.

#### 4.1.3 Estimates of vegetation-soil moisture coupling

To explore the relation between time-variable vegetation biases and estimates of vegetation-water coupling, we analysed the coefficient of determination  $R^2$  between  $\tau$  and soil moisture anomalies. These were derived from the SMOS  $\tau$  time series and



both SMAP and in-situ soil moisture, respectively. The associated anomalies  $\tau'$  and  $\theta'$  were obtained by subtracting a seasonal climatology that in turn was the smoothed (30 day) multi-year average of the input time series. To compare the SMAP and the in-situ soil moisture data, we then computed the difference in the coefficient of determination  $\Delta R^2$

$$\Delta R^2 = R^2(\tau'_{\text{SMOS}}, \theta'_{\text{SMAP}}) - R^2(\tau'_{\text{SMOS}}, \theta'_{\text{in-situ}}) \quad (8)$$

5 If the SMAP soil moisture were only contaminated by random noise relative to the in-situ data,  $\Delta R^2$  would tend to be negative. Time-variable vegetation biases, on the other hand, can induce positive values. Time-average biases cancel out. Of course, there are also other error sources such as representativeness errors, especially for the sparse networks. Further, the time series are comparatively short, but  $\Delta R^2$  can provide a first tentative assessment of the reliability of coupling metrics such as  $R^2$  in the presence of time-variable biases.

## 10 4.2 Results

### 4.2.1 Network sites

SMAP biases that track the vegetation misspecification  $\Delta\tau$  are common at the core validation sites. Especially changes in the sensitivity can be large.

The varying sensitivity is illustrated for the South Fork site, Iowa (USA), in Fig. 4a). In July, when the predominantly  
15 cultivated corn is heading and flowering (Tomer et al., 2008), the magnitude of the SMAP response to rainfall events matches that of the in-situ data. Conversely, in autumn (senescence, post harvest) the sensitivity of SMAP to soil moisture variations is diminished. The Bayesian inference reproduces this visually inferred pattern, as the sensitivity  $L$  drops by more than 0.5 (or 50%). By design, the temporal changes in  $L$  are governed by changes in  $\Delta\tau$ , which drops by about 0.1 from July to September. Over the entire time series, its temporal variability is  $|\lambda| = 0.3$ . Note that even when  $\Delta\tau \approx 0$  (August), the sensitivity is too  
20 low. As  $\Delta\tau$  is essentially zero on average over the entire time series (-0.006), the sensitivity at  $\Delta\tau = 0$  corresponds to the time-average value  $l$ . Its posterior median is 0.64 and thus less than the expected value of 1. We will return to the time-average biases later.

Pronounced changes in the sensitivity are found for all network sites but one (Fig. 4b). For the most part their magnitude is large, as the  $|\lambda|$  values correspond to a temporal variability of around 10 to 50%. The inferred relation to  $\Delta\tau$  is consistently  
25 positive ( $\lambda > 0$ ), i.e. as  $\Delta\tau$  increases over time, so does the SMAP sensitivity  $L(t)$ . The inferred direction hence matches the model prediction (Fig. 3a). The model does not constrain the magnitude of the  $\lambda$  parameter because the latter is an internally normalized quantity. When converted into absolute quantities ( $\lambda^*$ ), the inferred dependence of  $L$  on  $\Delta\tau$  matches the model predictions reasonably well (Fig. 4b).

Also the additive biases track changes in  $\Delta\tau$  at the network sites, but to a lesser extent (Fig. 4c). Over time, the biases vary  
30 by up to  $0.02 \text{ m}^3 \text{ m}^{-3}$  in magnitude. The inferred direction,  $\mu > 0$ , matches the predictions, as an increase in  $\Delta\tau$  corresponds to a larger offset. However, the magnitude of the inferred change of the offset with  $\Delta\tau$ ,  $\mu^*$ , is generally smaller than predicted. A very small value of  $\mu^*$  is found at the South Fork site: it is a factor of ten smaller than its predicted range (Fig. 4c). It is also small enough to be practically irrelevant, as the additive bias at South Fork is inferred to be essentially constant (Fig. 4a).

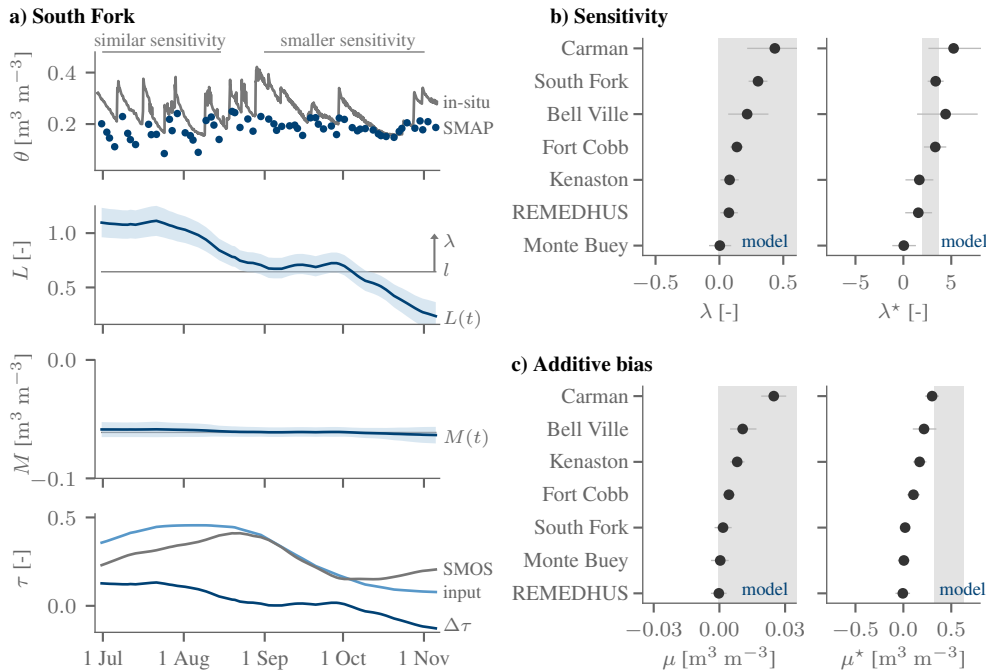


**Figure 4.** Time-variable biases over the network sites. a) The SMAP product’s sensitivity decreases from summer to late autumn 2015 at the South Fork site (42.4N, 93.4W), which is reflected by a decrease in the inferred sensitivity  $L$  that tracks a decrease in  $\Delta\tau$ : in early summer  $L(t) \approx 1$ , but it subsequently drops well below the time-average value of  $l = 0.7$ . Its temporal standard deviation is given by  $\lambda = 0.3$  (arrow).  $M(t)$  is approximately constant ( $M(t) \approx m$ ) because  $\mu$  is small (not shown). b) Over the network sites, the association of changes in the sensitivity with changes in  $\Delta\tau$  is predominantly positive ( $\lambda > 0$ ), as predicted by the model (marker: posterior median, lines: 5–95% uncertainty). The magnitude of the dependence for a unit change in  $\Delta\tau$ ,  $\lambda^*$ , is consistent with predictions by the  $\tau$ - $\omega$  model. c) The additive biases are of the right direction, but smaller than expected.

The time-variable biases are complemented by the time-average biases, which are quite large at several network sites. The time-average sensitivity  $l$  deviates from its nominal value of one by more than 30% at three out of 8 sites (Fig. 5). It tends to be larger than one, as may be expected considering the surface soil moisture SMAP is sensitive to has a larger dynamic range than at the depth of the probes. The South Fork site of (Fig. 4a) with  $l < 1$  is thus somewhat unusual. However, it is typical in that its time-average additive bias  $m$  is negative. Conversely, the noise level  $\sigma$  inferred using our approach tends to be small, usually on the order of  $0.03 \text{ m}^3 \text{ m}^{-3}$  (Fig. 5). These values are not directly comparable to standard RMSE estimates because our approach disentangles the quasi-random noise from a sensitivity that deviates from 1, temporally variable biases associated with  $\Delta\tau$  and in-situ errors. Also, the quasi-random errors tend to increase with  $\Delta\tau$  (Fig. 5), as predicted by the  $\tau$ - $\omega$  model (Fig. 3a). However, there is considerable variability in the magnitude across the study sites.

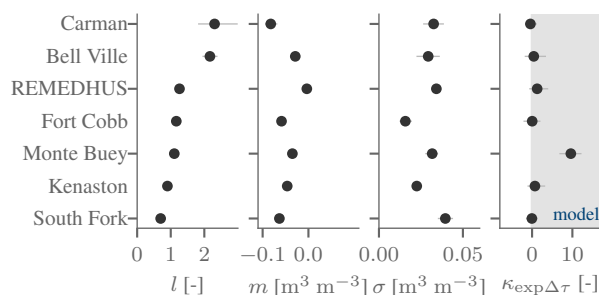


**Figure 5.** The time-average error properties  $l$  (sensitivity),  $m$  (additive bias) and  $\sigma$  (noise standard deviation), and the  $\kappa$  parameter (sensitivity of SMAP's noise level to  $\Delta\tau$ ) as inferred for all network sites. Meaning of markers and lines as in Fig. 4.

#### 4.2.2 Sensitivity analysis

The estimates of the time-variable biases are reasonably robust to the model specification. When the SMAP dual channel result is used as the reference  $\tau$  product, the bias parameters change little for the vast majority of sites (Fig. 6). By contrast, they can vary substantially when  $\tau$  is derived from contemporaneous NDVI data, indicating that the link between NDVI and  $\tau$ , rather than the use of a climatology, is a dominant error source in the SMAP vegetation input data. The impact of replacing the MERRA2 with the GLDAS2 soil moisture or dropping it altogether is also small (Fig. 6, columns 3 and 4). We also explored the sensitivity with respect to the model specification. When assuming homoscedastic errors (setting  $\kappa = 0$ ) or when allowing the soil moisture parameters  $A$  and  $B$  to vary seasonally (Eq. 5), the parameter estimates do not change substantially for all sites but one (Fig. 6, columns 5 and 6). The standard setup of the probabilistic model hence seems adequate for quantifying the SMAP error structure.

#### 4.2.3 Sparse sites

Across the sparse sites within the contiguous US we commonly find pronounced time-variable biases (Fig. 7a-b). While the results over the sparse sites are deemed much less reliable than those over the network sites, they are similar in areas of overlap. The largest changes in sensitivity of  $\lambda \approx 0.3$  are found over croplands (e.g. Midwest, Central Valley in California). As predicted by the model, the  $\lambda$  are predominantly positive but notable exceptions occur in the Mississippi Delta. Large and positive  $\lambda$  are also common over pastures and grasslands. The additive bias parameters  $\mu$  tend to show a similar spatial pattern, in that they are largest over crop- and grasslands (Fig. 7b). In summary, the sparse sites in agricultural regions reflect the results obtained over the network sites, and they reveal sizeable biases over grasslands in addition to croplands.

#### 4.2.4 Vegetation-soil moisture coupling

The observed coupling between vegetation and soil moisture anomalies is larger when using SMAP than when using in-situ soil moisture data (Fig. 7c). Positive values of  $\Delta R^2$  are particularly pronounced over croplands (0.12 on average), with the spatial pattern largely conforming to that of the time-variable biases. Conversely, if the time-variable errors in the remotely sensed

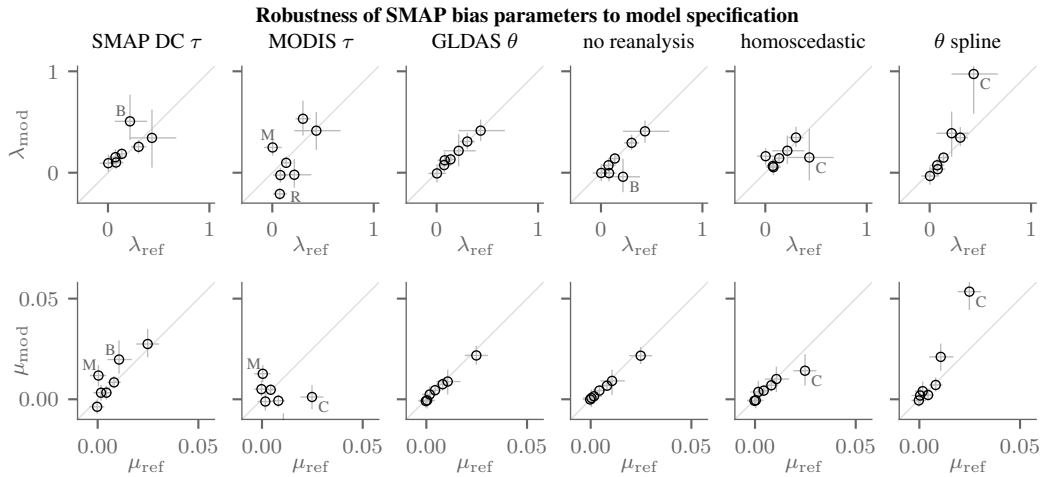


**Figure 6.** Robustness quantified by changes in the estimated  $\lambda$  (top row, [-]) and  $\mu$  (bottom row, [ $\text{m}^3 \text{m}^{-3}$ ]) parameters. Each panel compares the reference estimates on the horizontal axis (median: marker, lines: 10–90% posterior probability interval) to those obtained with the modified model on the vertical axis (cf. Sec. 4.1.2). The most prominent outliers are annotated – B: Bell Ville, C: Carman, M: Monte Buey, R: REMEDHUS.

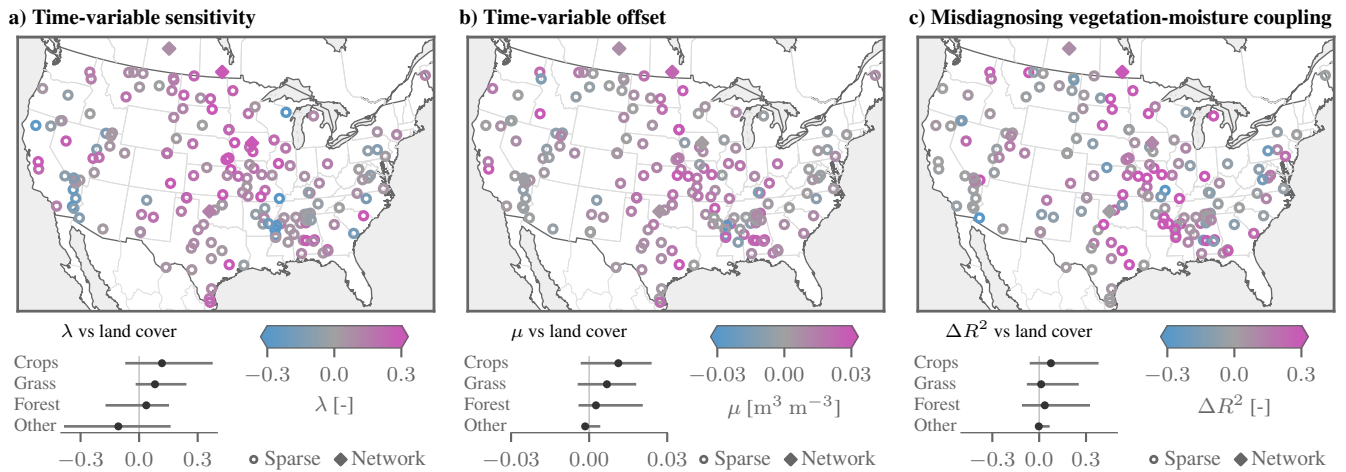


**Figure 7.** Time-variable biases and  $\Delta R^2$  coupling metric across the contiguous US, shown for the network sites and the sparse sites (only those with >250 valid SMAP observations). a) The time-dependent sensitivity parameters  $\lambda$  are predominantly positive, and the largest magnitudes are found over crop- and grasslands. b) The additive biases exhibit a similar spatial pattern. c) The degree of association  $R^2$  between anomalies of vegetation  $\tau$  (SMOS) and soil moisture is commonly higher for SMAP than for in-situ soil moisture ( $\Delta R^2 > 0$ ).





soil moisture were purely random, the degree of association would decrease, i.e.  $\Delta R^2 < 0$ . Even though spatial representative errors are likely large for the sparse networks, the  $\Delta R^2$  values are comparable at proximal network sites.

## 5 Discussion and conclusions

Soil moisture products can be subject to complex, time-variable errors, and we present a method for estimating such complex error structures from data. Other estimation procedures are conceivable, especially if high-quality in-situ data are available, and should be explored in the future. Our Bayesian triple collocation approach is widely applicable because it yields consistent estimates of error magnitude and biases even when no error-free reference soil moisture data set is available. It does, however, have to be assumed to be free of systematic error. The method is flexible, so that the error structure parameterization can be adapted to the problem at hand. We hope that this will enable the community to better characterize the uncertainties of remotely sensed soil moisture products. The knowledge of time-variable structural errors is key to improving the products, and it also helps to inform the application of these data sets in practice.

By applying the technique to the SMAP soil moisture product, we detect time-variable biases. These time-variable biases track the misspecification of the vegetation optical depth  $\Delta\tau$  during the soil moisture retrieval. They are both additive and multiplicative, i.e. not only the offset but also the sensitivity changes over time. Especially the changes in sensitivity can be large over croplands, as seasonal variations in  $L$  on the order of 30% ( $\lambda \approx 0.3$ ) deserve attention in future studies (Fig. 4, 7). The time-variable biases are relative to the in-situ data. The results over the sparse sites should hence be interpreted with caution due to representativeness error, even if they are similar to those at the dense high-quality network sites. Even at the network sites, residual time-dependent biases of the in-situ data cannot be ruled out completely.

The time-varying biases can be partially attributed to the imperfect vegetation correction during the retrieval. Their direction matches the theoretically predicted one (both  $\lambda$  and  $\mu$  are positive, Fig. 4). Also the magnitude of the change in sensitivity with a change in  $\Delta\tau$  is comparable to the predictions ( $\lambda^* \approx 3$ , Fig. 4b). However, the additive bias parameters  $\mu^*$  are too small (Fig. 4c). This may indicate insufficiencies in the input data such as the in-situ soil moisture or the reference vegetation optical depth, or the presence of partially compensating additional biases (e.g. confounding due to seasonal inundation).

One further caveat is that also time-average biases are present (additive bias:  $m \neq 0$ , sensitivity:  $l \neq 1$ ). For instance, the SMAP retrievals at the South Fork site have too low a sensitivity ( $l < 1$ ) and are too dry (negative  $m$ ) on average (Fig. 4a). Our analysis has focused on the time-dependent biases, partly because the time-independent biases are better known and more commonly compensated for in analyses such as data assimilation studies (Yilmaz and Crow, 2013; Kornelsen and Coulibaly, 2015; Colliander et al., 2017). Also, there are many potential sources for these time-invariant biases between the retrievals and the in-situ data, e.g. the calibration of the in-situ probes, the dielectric mixing model in the retrieval, or an offset in the mean input vegetation optical depth (i.e.  $\text{mean}(\Delta\tau) \neq 0$ ).

The time-varying biases can have a negative impact in many applications. The changing sensitivity impedes the seasonal comparison of soil moisture dynamics, as the same SMAP-observed change corresponds to a wide range of actual soil moisture changes depending on the season. Variable sensitivities are particularly problematic for characterizing droughts, as extreme



5 conditions may not be apparent in the SMAP data when the sensitivity happens to be small at the time. Further, the spurious  
vegetation signal in the soil moisture data can distort estimates of water-vegetation coupling. We find inflated values of  $R^2$   
between the SMOS vegetation optical depth and SMAP soil moisture, whereas purely random noise would decrease the  $R^2$   
(Fig. 7c). Even though these results are only preliminary due to the limited time span, they underscore potential pitfalls in  
studies of global hydrology.

Our findings illustrate the importance of recognizing time-variable biases in general. The uncertainty analyses, including  
the choice of metrics or error parameters, must account for them. The widely used RMSE cannot distinguish between such  
systematic errors and white noise. Neglecting that distinction can easily give rise to misleading interpretations, for instance into  
how water availability regulates land surface processes. For illustration, consider its phenology-dependent role in transpiration  
and plant growth. Remotely sensed soil moisture products provide unique insight into these couplings, but only up to a point as  
phenology-dependent biases of unknown size are potentially present in all remotely sensed products. Neglecting the associated  
seasonal and inter-annual biases will distort observation-based estimates of the couplings. Robust estimates of such complex  
error structures can help to mitigate these biases, and thus to exploit the full potential of observational data sets.

## 6 Acknowledgements

15 The authors are grateful to Kaighin McColl, Dara Entekhabi and his group, and the SMAP team for comments and sug-  
gestions. S.Z. acknowledges support from the Swiss National Science Foundation (P2EZP2\_168789). The support of the  
Canadian Space Agency, Environment and Climate Change Canada and the Natural Sciences and Engineering Research  
Council of Canada is acknowledge for support of the Kenaston network. A contribution to this work was made at the Jet  
Propulsion Laboratory, California Institute of Technology, under a contract with the National Aeronautics and Space Admin-  
20 istration. The University of Salamanca team's involvement in this study was supported by the Spanish Ministry of Econ-  
omy and Competitiveness with the project PROMISES: ESP2015-67549-C3 and the European Regional Development Fund  
(ERDF). The remotely sensed and reanalysis data are available at the URLs provided in the references (registration generally  
required). The sparse in-situ data can be found at *ismn.geo.tuwien.ac.at*. The SMAP network in-situ data are available from  
<https://nsidc.org/data/nsidc-0712> until October 2016; the 2017 data are expected to be uploaded in early 2018; until then,  
25 they are available from the authors upon request. The Python code for Bayesian triple collocation has been made available at  
<https://github.com/szwieback/BayesianTripleCollocation>.



## References

- Adegoke, J. O. and Carleton, A. M.: Relations between Soil Moisture and Satellite Vegetation Indices in the U.S. Corn Belt, *Journal of Hydrometeorology*, 3, 395–405, [https://doi.org/10.1175/1525-7541\(2002\)003<0395:RBSMAS>2.0.CO;2](https://doi.org/10.1175/1525-7541(2002)003<0395:RBSMAS>2.0.CO;2), 2002.
- Al Bitar, A., Mialon, A., Kerr, Y. H., Cabot, F., Richaume, P., Jacquette, E., Quesney, A., Mahmoodi, A., Tarot, S., Parrens, M., Al-Yaari, A., Pellarin, T., Rodriguez-Fernandez, N., and Wigneron, J.-P.: The global SMOS Level 3 daily soil moisture and brightness temperature maps, *Earth System Science Data*, 9, 293–315, <https://doi.org/10.5194/essd-9-293-2017>, 2017.
- Bell, J. E., Palecki, M. A., Baker, C. B., Collins, W. G., Lawrimore, J. H., Leeper, R. D., Hall, M. E., Kochendorfer, J., Meyers, T. P., Wilson, T., and Diamond, H. J.: U.S. Climate Reference Network Soil Moisture and Temperature Observations, *Journal of Hydrometeorology*, 14, 977–988, <https://doi.org/10.1175/JHM-D-12-0146.1>, 2013.
- Brooks, S. P. and Gelman, A.: General Methods for Monitoring Convergence of Iterative Simulations, *Journal of Computational and Graphical Statistics*, 7, 434–455, <https://doi.org/10.1080/10618600.1998.10474787>, 1998.
- Chan, S., Bindlish, R., O'Neill, P., Jackson, T., Njoku, E., Dunbar, S., Chaubell, J., Piepmeier, J., Yueh, S., Entekhabi, D., Colliander, A., Chen, F., Cosh, M., Caldwell, T., Walker, J., Berg, A., McNairn, H., Thibeault, M., Martínez-Fernández, J., Uldall, F., Seyfried, M., Bosch, D., Starks, P., Collins, C. H., Prueger, J., van der Velde, R., Asanuma, J., Palecki, M., Small, E., Zreda, M., Calvet, J., Crow, W., and Kerr, Y.: Development and assessment of the SMAP enhanced passive soil moisture product, *Remote Sensing of Environment*, pp. –, <https://doi.org/10.1016/j.rse.2017.08.025>, 2017.
- Chan, S. K., Bindlish, R., O'Neill, P. E., Njoku, E., Jackson, T., Colliander, A., Chen, F., Burgin, M., Dunbar, S., Piepmeier, J., Yueh, S., Entekhabi, D., Cosh, M. H., Caldwell, T., Walker, J., Wu, X., Berg, A., Rowlandson, T., Pacheco, A., McNairn, H., Thibeault, M., Martínez-Fernández, J., González-Zamora, ., Seyfried, M., Bosch, D., Starks, P., Goodrich, D., Prueger, J., Palecki, M., Small, E. E., Zreda, M., Calvet, J. C., Crow, W. T., and Kerr, Y.: Assessment of the SMAP Passive Soil Moisture Product, *IEEE Transactions on Geoscience and Remote Sensing*, 54, 4994–5007, <https://doi.org/10.1109/TGRS.2016.2561938>, 2016.
- Colliander, A.: SMAP/In Situ Core Validation Site Land Surface Parameters Match-Up Data, Version 1, NASA National Snow and Ice Data Center Distributed Active Archive Center, <https://doi.org/10.5067/DXAVIXLY18KM>, 2017.
- Colliander, A., Jackson, T., Bindlish, R., Chan, S., Das, N., Kim, S., Cosh, M., Dunbar, R., Dang, L., Pashaian, L., Asanuma, J., Aida, K., Berg, A., Rowlandson, T., Bosch, D., Caldwell, T., Caylor, K., Goodrich, D., al Jassar, H., Lopez-Baeza, E., Martínez-Fernández, J., González-Zamora, A., Livingston, S., McNairn, H., Pacheco, A., Moghaddam, M., Montzka, C., Notarnicola, C., Niedrist, G., Pellarin, T., Prueger, J., Pulliainen, J., Rautiainen, K., Ramos, J., Seyfried, M., Starks, P., Su, Z., Zeng, Y., van der Velde, R., Thibeault, M., Dorigo, W., Vreugdenhil, M., Walker, J., Wu, X., Monerris, A., O'Neill, P., Entekhabi, D., Njoku, E., and Yueh, S.: Validation of SMAP surface soil moisture products with core validation sites, *Remote Sensing of Environment*, 191, 215 – 231, <https://doi.org/http://dx.doi.org/10.1016/j.rse.2017.01.021>, 2017.
- Diamond, H. J., Karl, T. R., Palecki, M. A., Baker, C. B., Bell, J. E., Leeper, R. D., Easterling, D. R., Lawrimore, J. H., Meyers, T. P., Helfert, M. R., Goodge, G., and Thorne, P. W.: U.S. Climate Reference Network after One Decade of Operations: Status and Assessment, *Bulletin of the American Meteorological Society*, 94, 485–498, <https://doi.org/10.1175/BAMS-D-12-00170.1>, 2013.
- Didan, K.: MYD13A2: MODIS/Aqua Vegetation Indices 16-Day L3 Global 1 km SIN Grid V006, <https://doi.org/10.5067/MODIS/MYD13A2.006>, <https://lpdaac.usgs.gov/>, accessed 30 September 2017, 2017.
- Doherty, J. and Welter, D.: A short exploration of structural noise, *Water Resources Research*, 46, n/a–n/a, <https://doi.org/10.1029/2009WR008377>, w05525, 2010.



- Dorigo, W., Wagner, W., Albergel, C., Albrecht, F., Balsamo, G., Brocca, L., Chung, D., Ertl, M., Forkel, M., Gruber, A., Haas, E., Hamer, P. D., Hirschi, M., Ikonen, J., de Jeu, R., Kidd, R., Lahoz, W., Liu, Y. Y., Miralles, D., Mistelbauer, T., Nicolai-Shaw, N., Parinussa, R., Pratola, C., Reimer, C., van der Schalie, R., Seneviratne, S. I., Smolander, T., and Lecomte, P.: ESA CCI Soil Moisture for improved Earth system understanding: State-of-the art and future directions, *Remote Sensing of Environment*, <https://doi.org/10.1016/j.rse.2017.07.001>, 2017.
- Entekhabi, D., Reichle, R., Koster, R., and Crow, W.: Performance Metrics for Soil Moisture Retrievals and Application Requirements, *J. Hydrometeorol.*, 11, 832–840, 2010.
- Friedl, m., Menashe-Sulla, D., and MOSAPS SIPS: MCD12C1 MODIS/Terra+Aqua Land Cover Type Yearly L3 Global 0.05Deg CMG, NASA LP DAAC, <https://doi.org/10.5067/MODIS/MCD12C1.006>, accessed: 10 October 2017, 2017.
- 10 Gelaro, R., McCarty, W., Suárez, M. J., Todling, R., Molod, A., Takacs, L., Randles, C. A., Darmenov, A., Bosilovich, M. G., Reichle, R., Wargan, K., Coy, L., Cullather, R., Draper, C., Akella, S., Buchard, V., Conaty, A., da Silva, A. M., Gu, W., Kim, G.-K., Koster, R., Lucchesi, R., Merkova, D., Nielsen, J. E., Partyka, G., Pawson, S., Putman, W., Rienecker, M., Schubert, S. D., Sienkiewicz, M., and Zhao, B.: The Modern-Era Retrospective Analysis for Research and Applications, Version 2 (MERRA-2), *Journal of Climate*, 30, 5419–5454, <https://doi.org/10.1175/JCLI-D-16-0758.1>, 2017.
- 15 Gelman, A., Jakulin, A., Pittau, M. G., and Su, Y.-S.: A Weakly Informative Default Prior Distribution for Logistic and Other Regression Models, *The Annals of Applied Statistics*, 2, 1360–1383, 2008.
- Global Modeling and Assimilation Office: MERRA-2 tavg1\_2d\_ind\_nx: 2d,1-Hourly,Time-Averaged,Single-Level,Assimilation,Land Surface Diagnostics V5.12.4, Goddard Earth Sciences Data and Information Services Center, <https://doi.org/10.5067/RKPHT8KC1Y1T>, [https://disc.gsfc.nasa.gov/datasets/M2T1NXLND\\_V5.12.4/](https://disc.gsfc.nasa.gov/datasets/M2T1NXLND_V5.12.4/), accessed on 14 September 2017, 2017.
- 20 Gruber, A., Su, C.-H., Zwieback, S., Crow, W., Dorigo, W., and Wagner, W.: Recent advances in (soil moisture) triple collocation analysis, *International Journal of Applied Earth Observation and Geoinformation*, 45, 200 – 211, <https://doi.org/10.1016/j.jag.2015.09.002>, 2016.
- Harvey, A. C.: Estimating regression models with multiplicative heteroscedasticity, *Econometrica*, 44, 461–465, 1976.
- Hoffman, M. and Gelman, A.: The No-U-Turn sampler: Adaptively setting path lengths in Hamiltonian Monte Carlo, *Journal of Machine Learning Research*, 15, 1351–1381, 2014.
- 25 Konings, A. G., Piles, M., Das, N., and Entekhabi, D.: L-band vegetation optical depth and effective scattering albedo estimation from SMAP, *Remote Sensing of Environment*, 198, 460 – 470, <https://doi.org/http://dx.doi.org/10.1016/j.rse.2017.06.037>, 2017.
- Kornelsen, K. and Coulibaly, P.: Reducing multiplicative bias of satellite soil moisture retrievals, *Remote Sensing of Environment*, 165, 109 – 122, <https://doi.org/10.1016/j.rse.2015.04.031>, 2015.
- Kurum, M., Lang, R. H., O’Neill, P. E., Joseph, A. T., Jackson, T. J., and Cosh, M. H.: A First-Order Radiative Transfer Model for Microwave Radiometry of Forest Canopies at L-Band, *IEEE Transactions on Geoscience and Remote Sensing*, 49, 3167–3179, <https://doi.org/10.1109/TGRS.2010.2091139>, 2011.
- 30 Lawrence, H., Wigneron, J.-P., Richaume, P., Novello, N., Grant, J., Mialon, A., Bitar, A. A., Merlin, O., Guyon, D., Leroux, D., Bircher, S., and Kerr, Y.: Comparison between SMOS Vegetation Optical Depth products and MODIS vegetation indices over crop zones of the USA, *Remote Sensing of Environment*, 140, 396 – 406, <https://doi.org/http://dx.doi.org/10.1016/j.rse.2013.07.021>, 2014.
- 35 Loew, A. and Schlenz, F.: A dynamic approach for evaluating coarse scale satellite soil moisture products, *Hydrology and Earth System Sciences*, 15, 75–90, <https://doi.org/10.5194/hess-15-75-2011>, 2011.
- MacKay, D. J. C.: *Information Theory, Inference, and Learning Algorithms*, Cambridge University Press, 2003.



- O' Neill, P., Chan, S., Njoku, E., Jackson, T., and Bindlish, R.: SMAP Enhanced L2 Radiometer Half-Orbit 9 km EASE-Grid Soil Moisture, Version 1., NASA National Snow and Ice Data Center Distributed Active Archive Center, <https://doi.org/10.5067/CE0K6JS5WQMM>, [https://nsidc.org/data/SPL2SMP\\_E](https://nsidc.org/data/SPL2SMP_E), accessed on 25 August 2017.
- Palecki, M., Lawrimore, J., Leeper, R., Bell, J., Embler, S., and Casey, N.: U.S. Climate Reference Network Processed Data from USCRN Database Version 2, National Centers for Environmental Information, NESDIS, NOAA, U.S. Department of Commerce, <https://doi.org/doi:10.7289/V5MS3QR9>, 2017.
- Patton, J. and Hornbuckle, B.: Initial Validation of SMOS Vegetation Optical Thickness in Iowa, *IEEE Geoscience and Remote Sensing Letters*, 10, 647–651, <https://doi.org/10.1109/LGRS.2012.2216498>, 2013.
- Roddell, M. and Beaudoin, H.: GLDAS Noah Land Surface Model L4 3 hourly 0.25 x 0.25 degree V2.1, NASA GESDISC DATA ARCHIVE, <https://doi.org/10.5067/E7TYRXPJKWOQ>, [https://hydro1.gesdisc.eosdis.nasa.gov/data/GLDAS/GLDAS\\_NOAH025\\_3H.2.1/](https://hydro1.gesdisc.eosdis.nasa.gov/data/GLDAS/GLDAS_NOAH025_3H.2.1/), accessed 30 September 2017, 2017.
- Salvatier, J., Wiecki, T. V., and Fonnesbeck, C.: Probabilistic programming in Python using PyMC3, *PeerJ Computer Science*, 2, e55, <https://doi.org/10.7717/peerj-cs.55>, 2016.
- Schaefer, G. L., Cosh, M. H., and Jackson, T. J.: The USDA Natural Resources Conservation Service Soil Climate Analysis Network (SCAN), *Journal of Atmospheric and Oceanic Technology*, 24, 2073–2077, <https://doi.org/10.1175/2007JTECHA930.1>, <https://doi.org/10.1175/2007JTECHA930.1>, 2007.
- Su, C.-H. and Ryu, D.: Multi-scale analysis of bias correction of soil moisture, *Hydrology and Earth System Sciences*, 19, 17–31, <https://doi.org/10.5194/hess-19-17-2015>, 2015.
- Su, C.-H., Ryu, D., Dorigo, W., Zwieback, S., Gruber, A., Albergel, C., Reichle, R. H., and Wagner, W.: Homogeneity of a global multi-satellite soil moisture climate data record, *Geophysical Research Letters*, 43, 11,245–11,252, <https://doi.org/10.1002/2016GL070458>, 2016GL070458, 2016.
- Tomer, M., Moorman, T., and Rossi, C.: Assessment of the Iowa River's South Fork watershed: Part 1. Water quality, *Journal of Soil and Water Conservation*, 63, 360–370, 2008.
- Xu, T., Valocchi, A. J., Ye, M., and Liang, F.: Quantifying model structural error: Efficient Bayesian calibration of a regional groundwater flow model using surrogates and a data-driven error model, *Water Resources Research*, 53, 4084–4105, <https://doi.org/10.1002/2016WR019831>, 2017.
- Yilmaz, M. T. and Crow, W. T.: The Optimality of Potential Rescaling Approaches in Land Data Assimilation, *Journal of Hydrometeorology*, 14, 650–660, <https://doi.org/10.1175/JHM-D-12-052.1>, 2013.
- Zwieback, S., Scipal, K., Dorigo, W., and Wagner, W.: Structural and statistical properties of the collocation technique for error characterization, *Nonlin. Processes Geophys.*, 19, 69–80, 2012.
- Zwieback, S., Su, C.-H., Gruber, A., Dorigo, W. A., and Wagner, W.: The Impact of Quadratic Nonlinear Relations between Soil Moisture Products on Uncertainty Estimates from Triple Collocation Analysis and Two Quadratic Extensions, *Journal of Hydrometeorology*, 17, 1725–1743, <https://doi.org/10.1175/JHM-D-15-0213.1>, 2016.